Understanding the relationships between heterogeneous microstructures and tensile properties through characterization of plastic strain localization in ti-6al-4v processed by wded.

François Bourdin, S. Lopez Castaño, Samuel Hémery, Damien Texier, Florence Pettinari-Sturmel, Joël Douin, C. Archambeau, P. Emile

▶ **To cite this version:**

François Bourdin, S. Lopez Castaño, Samuel Hémery, Damien Texier, Florence Pettinari-Sturmel, et al.. Understanding the relationships between heterogeneous microstructures and tensile properties through characterization of plastic strain localization in ti-6al-4v processed by wded.. Ti-2023-World Titanium Conference 2023, Jun 2023, Edinburgh, United Kingdom. hal-04167968

HAL Id: hal-04167968
https://imt-mines-albi.hal.science/hal-04167968v1

Submitted on 24 Jul 2023

HAL is a multi-disciplinary open access archive for the deposit and dissemination of scientific research documents, whether they are published or not. The documents may come from teaching and research institutions in France or abroad, or from public or private research centers.

L'archive ouverte pluridisciplinaire **HAL**, est destinée au dépôt et à la diffusion de documents scientifiques de niveau recherche, publiés ou non, émanant des établissements d'enseignement et de recherche français ou étrangers, des laboratoires publics ou privés.

UNDERSTANDING THE RELATIONSHIPS BETWEEN HETEROGENEOUS MICROSTRUCTURES AND TENSILE PROPERTIES THROUGH CHARACTERIZATION OF PLASTIC STRAIN LOCALIZATION IN TI-6AL-4V PROCESSED BY WDED.

F. Bourdin[1,2], S. Lopez Castaño[3,4], S. Hemery[5], D. Texier[1], F. Pettinari-Sturmel[3], J. Douin[3], C. Archambeau[4], P. Emile[4]

1 Institut Clément Ader (ICA) – UMR CNRS 5312 ; Université de Toulouse ; CNRS, IMT Mines Albi, INSA, ISAE-SUPAERO, UPS ; Albi, France.
2 Airbus Central R&T, 2 rond-point Emile Dewoitine, 31 703, Blagnac, France
3 CEMES, 29 rue Jeanne Marvig, 31 055, Toulouse, France
4 Airbus Operations SAS, 316 route de Bayonne, 31 060, Toulouse, France
5 Institut Pprime, ISAE-ENSMA, Université de Poitiers, CNRS UPR 3346, Téléport 2, 1 avenue Clément Ader, BP40109, Futuroscope Chasseneuil Cedex, 86 961, France

Wire Direct Energy Deposition (WDED) processes enable near-net-shape manufacturing with a high deposition rate and improved size capabilities as compared to powder-based additive manufacturing (AM) processes. They can be classified according to the employed heat source: a beam, either laser for Wire Laser AM (WLAM) or electron for Electron Beam AM (EBAM), or an arc welding for Wire Arc AM (WAAM). Prior studies have enabled us to limit the introduction of defects and contamination issues using WDED technologies. However, the process-inherited heterogeneous microstructures, including strong crystallographic textures, and consequences on anisotropy and variability in mechanical properties are still not fully understood. In particular, Heat Affected Zones (HAZ) are clearly observed in the material and their features are strongly related to the heat source and the scanning strategy. These HAZ are known to produce a highly heterogeneous microstructure at the millimetre scale with a gradient of α-lath thickness and clusters of crystallographic variants. While these areas are prone to a heterogeneous strain distribution, the relation with macroscopic ductility remains unclear for WDED processes. In the present work, deformation heterogeneity was studied in relation to microstructure to clarify the role of the HAZ-induced strain localization on tensile anisotropy. Digital image correlation (DIC) combined with electron back-scattered diffraction (EBSD) was employed for this purpose. In particular, spatial variations in lamella thickness and implications of Burgers Orientation Relationships were considered to understand the heterogeneous development of slip activity.

Keywords: Ti64, Wire Direct Energy Deposition (W-DED), Wire Laser Additive Manufacturing (WLAM), Wire Arc Additive Manufacturing (WAAM) - CMT (Cold Metal Transfer), Electron Beam Additive Manufacturing (EBAM)

1. Introduction

The perpetual quest for weight saving, cost reduction (Buy-To-Fly) and improved environmental footprint has led the aerospace industry to take a closer look at Wire Direct Energy Deposition (WDED). WDED is a near-net-shape process whose main driver is to enable a dramatic increase in deposition rate and size capabilities compared to powder-based AM. Besides, it could shorten drastically part development cycle while saving materials and energy, compared with conventional processes [1, 13].

WDED processes can be classified in two main categories according to their heat source: using a beam (Laser for WLAM or Electron for EBAM), or an Arc for WAAM. Once defects & contamination problems are mastered, the key challenge in WDED technologies is the heterogeneous microstructure associated with strong crystallographic texture and high anisotropy in mechanical properties [1, 2, 8, 9]. To improve deposited microstructure, different approaches are currently developed: in-process deformation, chemical inoculation, high intensity ultrasound and advanced process control (Cold Metal Transfer (CMT), coaxial beam, etc ...) [3-7].

WDED printed Ti–6Al–4V materials possess the following typical characteristics: large columnar β grains, an α-transformation texture inherited from the β-solidification texture, a periodic Heat Affected Zone (HAZ) arranged in a banded microstructure; each band being composed of a variety of α microstructures ranging from fine to coarse Widmanstätten, α-grain boundary (αGB) and α-colonies.

The HAZ produced during the process can have a significant impact on the microstructure of the material, which in turn can lead to strain variability in strain localization in the final part. This proceeding will explore the effect of HAZ on microstructure and strain localization in 3 WDED processes: WAAM-CMT, WLAM coaxial beam and EBAM. The intricate relation between the local mechanical behavior and such heterogeneous microstructures is investigated using DIC coupled with EBSD. These investigations aim to identify the main parameters piloting mechanical behavior and to better understand macroscopic mechanical anisotropy.

2. Materials and methods

2.1. TA6V wall printing

Two Ti-6Al-4V walls were printed at ADDIMADOUR ESTIA inside an inert chamber with a WAAM-CMT Fronius Transpul Synergic CMT TPS3200 robotic cell and a WLAM Precitec Coaxial beam robotic cell. These walls were printed from a 1.2 mm-diameter AMS4954 TA6V wire on an AMS4911 substrate. The WAAM-CMT and WLAM wall were printed with an

alternating oscillation and a contouring trig edge strategy respectively.

The EBAM wall was printed in a vacuum chamber with a Sciaky EBAM 110 printer in Airbus St Eloi from a 3.2 mm-diameter TA6V wire on an AMS4911 substrate. The wall was printed using a single-track strategy.

All walls were finally heat treated so as to relieve internal stresses accumulated throughout the printing process.

2.2. *Mechanical testing*

Macroscopic quasi-static tension tests were performed according to ASTME8 at room temperature using a cylindrical specimen geometry. The symbolic legend corresponding to the specimen positions are presented in Figure 1. Three directions are tested (BD, 45BD, LD) for WLAM and WAAM-CMT and the BD direction is tested at the 2 extremities. The EBAM is tested along the BD and LD directions only. The substrate plate is also tested for comparison. Each direction is tested with 3 specimens.

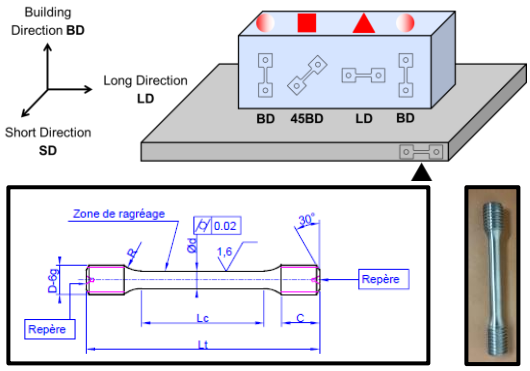

Figure 1. Schematic illustration of the micro-tensile specimen locations and macroscopic specimen geometry.

2.3. *Micro-mechanical testing coupled with DIC*

Micro-tensile tests were performed *in-situ* at room temperature using a 5kN Deben test rig using a 0.05 mm/min crosshead displacement rate under a Zeiss AXIO Imager Optical Microscope (OM) on flat dog-bone specimens, as illustrated on Figure 2. Specimens were extracted along the Building Direction (BD). They are prepared according to the protocol described by Yvinec and Lunt [9, 10]. The final Kroll etching step allows to produce a fine speckle to perform Digital Image Correlation (DIC) under OM. A stitched grid of 9 × 3 images is acquired with a resolution of 1.46 px/µm. The DIC calculation is performed on NCorr V1.2 with a subset and step size of 32 px and 8 px respectively. The tensile test was interrupted at 4 strain increments: 0.00015 %; 0.61 %; 1.35 % and 3.2 %.

This DIC technique allows to access 2D plane strain components at grain level with Optical Microscope resolution. Other techniques such as Laser Scanning Confocal Microscopy (LSCM) enable to access the out-of-plane component [12, 14].

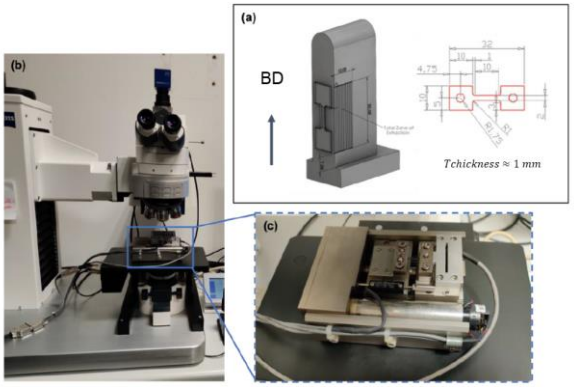

Figure 2. (a) Specimen geometry and sampling in the EBAM wall. (b and c) micro-machine test rig under a Zeiss AXIO Imager.

2.4. *Chemical analysis*

The chemical analysis has been conducted according to ASTME1409, ASTME1041 and ASTME2371 on parallelepiped specimen sampled at the top of the different walls.

2.5. *Microstructure analysis with EBSD*

Microstructural analysis was carried out on specimens mechanically ground with SiC paper up to P4000 grit. A polishing step involving a 9 µm diamond suspension was applied before finishing with a mixture of 10% hydrogen peroxide and 90% colloidal silica solution containing 0.04 µm particles.

Crystallographic orientations were characterized using EBSD with a step size ranging from 0.8 µm to 3 µm adapted to the different microstructure size.

3. Results

3.1. *Macroscopic Tensile and chemical results*

Tensile properties are summarized in Figure 3 with several AMS specifications (AMS 4928R forged αβ, AMS 4911 αβ plate, AMS 4905D β plate), plotted in dotted lines. It highlights a clear mechanical anisotropy with the highest UTS and $YS_{0.2}$ along 45BD direction and the lowest UTS and $YS_{0.2}$ along BD. In terms of elongation, BD has the maximum value for the 3 walls. Besides both ends of the walls display similar mechanical properties. These observations are consistent with literature [2].

From a WDED point of view, the WAAM-CMT has the highest UTS and $YS_{0.2}$ but low ductility in all directions which does not meet AMS specifications. EBAM meets almost all AMS standards except on BD direction. WLAM presents interesting results as it meets all AMS standards shown here and exhibited a good mechanical property in all directions tested.

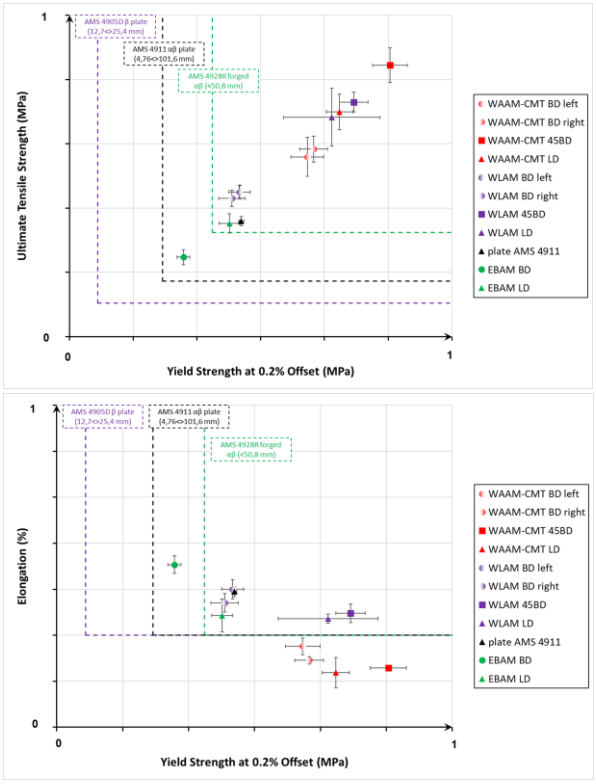

Figure 3. UTS versus $YS_{0.2}$ and Elongation versus $YS_{0.2}$ for WAAM-CMT, WLAM and EBAM. Several AMS standards are plotted in dotted lines.

The chemical results are given in Table 1. First observation underlines the oxygen and nitrogen uptake above 0.2 wt.% for the WAAM-CMT, which can explain the difference in mechanical properties. The 2 other walls have nominal concentration of element, however EBAM shows the lowest Aluminium concentration.

Table 1: Chemical composition (wt. %) of the different WDED wall TA6V.

WDED	Al	V	Fe	C	O	N	H
EBAM	**5,72**	4,04	0,20	0,03	**0,15**	0,01	<0.01
WAAM-CMT	**5,96**	3,93	0,17	0,02	**0,21**	0,05	<0.01
WLAM	**6,14**	3,88	0,17	0,01	**0,17**	0,01	<0.01

3.2. Microstructural analyses

The microstructure of the 3 walls in the BD-SD plane are presented on Figure 4. The EBSD maps show a clear difference in size from the coarsest to the finest microstructures deposited in the EBAM, WAAM-CMT and WLAM walls respectively. Thus, the CMT and coaxial Laser approaches succeeded in producing finer microstructure through a better heat control.

A zoom on a HAZ band in the WAAM-CMT shows the complex α microstructures generated including fine to coarse Widmanstätten, α-grain boundary (αGB) and α-colonies. This highly heterogeneous α-microstructure at HAZ described by Ho [11] is observed in all the studied walls.

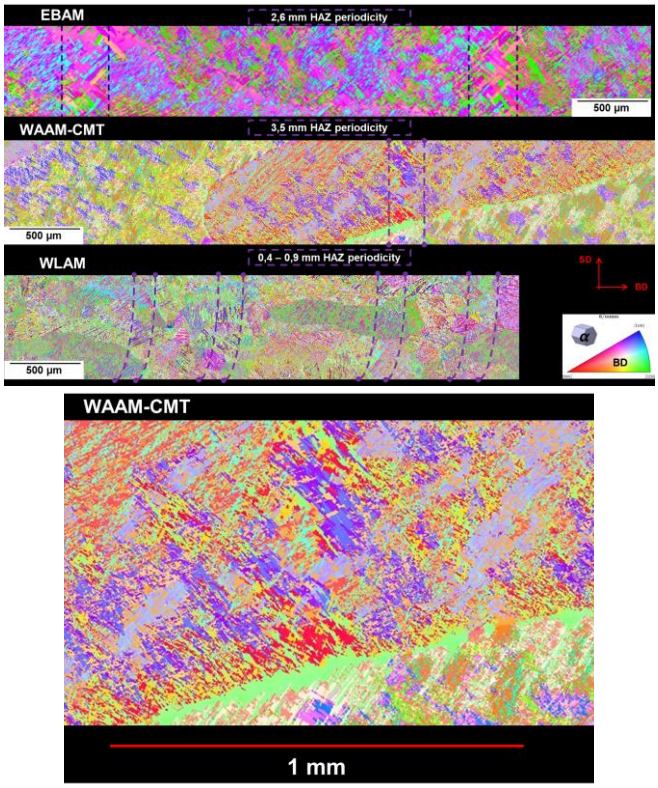

Figure 4. Inverse Pole Figure maps of EBAM, WLAM and WAAM-CMT in the BD-SD plane with crystallographic orientations along BD. HAZ bands are highlighted with purple dotted lines. Zoom in the HAZ in the WAAM-CMT.

3.3. Strain localization at HAZ on EBAM along BD

The correlative analysis conducted on EBAM tested along BD is illustrated on Figure 5. First, the strain map shows a heterogeneous strain development. A noticeable correlation between the HAZ band or the prior β grain boundary and local strain values is observed. The lowest strain values are located on the right handside the HAZ bands and highest strain values are located on the left handside. Although further investigations are needed

to clarify the relationships between the intricate microstructure and the heterogeneous deformation, this suggests that regions with refined α laths display lower plastic strain levels.-This is consistent with the well-known strengthening effect provided by a high density of interfaces.

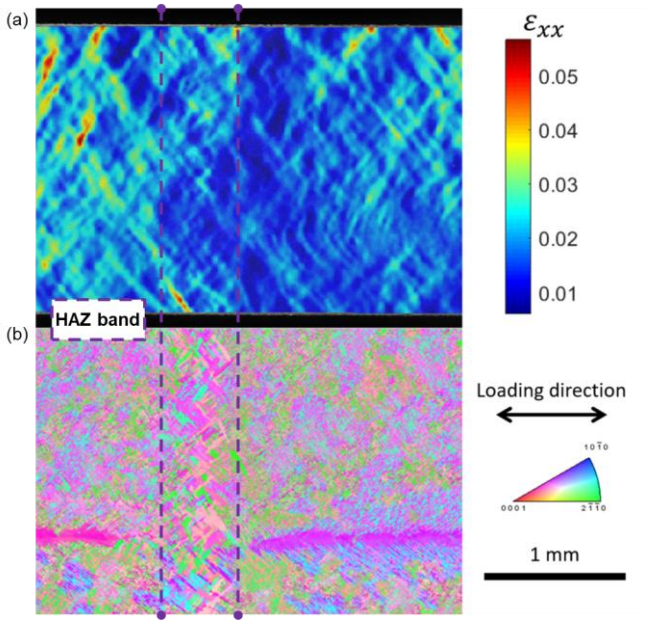

Figure 5. (a) ε_{xx} strain and (b) Inverse Pole Figure map coded along BD of a region containing a HAZ band and a prior β grain boundary at a 3.2 % macroscopic strain .

4. Conclusions

Three WDED processes have been studied in terms of mechanical and microstructural properties. Mechanical anisotropy is demonstrated in all the walls with the highest elongation obtained along the BD direction. The main difference lies in the global microstructure size which is coarser for the EBAM compared to WAAM-CMT and WLAM. In all the walls, a highly heterogeneous α microstructure is observed in relation to HAZ.

To deepen the analysis, a micro-mechanical approach coupling DIC and EBSD has been conducted. The analysis on EBAM along BD shows an important effect of microstructural features including prior β grain boundaries and HAZ bands on strain localization.

This feature is under on-going investigation. However, the results from this study will provide valuable insights in terms of microstructure – mechanical behavior, and could lead to the development of new strategies to improve the quality and reliability of parts produced using WDED.

5. Acknowledgements

The authors would like to thank Pierre Michaud and Anaïs Domergue from Addimadour ESTIA for printing WLAM and WAAM-CMT walls. Dassault Aviation, Airbus and “France Relance” program are kindly acknowledged for financial support.

6. References

1. Herzog, D., Seyda, V., Wycisk, E., & Emmelmann, C. (2016). Additive manufacturing of metals. *Acta Materialia*, *117*, 371-392.
2. WAAM mechanical properties Through the WAAMMat Programme, 2019, S. Williams
3. Kennedy, J. R., Davis, A. E., Caballero, A. E., Williams, S., Pickering, E. J., & Prangnell, P. B. (2021). The potential for grain refinement of Wire-Arc Additive Manufactured (WAAM) Ti-6Al-4V by ZrN and TiN inoculation. Additive Manufacturing, 40, 101928., Proceeding Titanium
4. Todaro, C. J., et al. "Grain structure control during metal 3D printing by high-intensity ultrasound." Nature communications 11.1 (2020): 142.
5. Colegrove, P.A., Martina, F., Roy, M.J., Szost, B., Terzi, S., Williams, S.W., Withers, P.J., Jarvis, D., 2014. High pressure interpassrolling of Wire + Arc Additively Manufactured titanium components. Advanced Materials Research 996, 694–700.
6. Davis, A. E., Kennedy, J. R., Strong, D., Kovalchuk, D., Porter, S., & Prangnell, P. B. (2021). Tailoring equiaxed β-grain structures in Ti-6Al-4V coaxial electron beam wire additive manufacturing. Materialia, 20, 101202.
7. Donoghue, J., Antonysamy, A. A., Martina, F., Colegrove, P. A., Williams, S. W., & Prangnell, P. B. (2016). The effectiveness of combining rolling deformation with Wire–Arc Additive Manufacture on β-grain refinement and texture modification in Ti–6Al–4V. Materials Characterization, 114, 103-114.
8. S. Lopez Castano, Optimization of static properties of Ti-6Al-4V obtained by Wire-Direct Energy Deposition via a multi-scale analysis of the microstructure, PhD manuscript.
9. D. Lunt, et al., “The effect of loading direction on strain localization in wire arc additively manufactured Ti–6Al–4V”, Mater. Sci. Eng. A 788 (2020)
10. Yvinec, T., Naït-Ali, A., Mellier, D., Bertheau, D., Cormier, J., Villechaise, P., ... & Hémery, S. (2022). Tensile properties of Ti-6Al-4V as-built by laser metal deposition: The relationship between heat affected zone bands, strain localization and anisotropy in ductility. Additive Manufacturing, 55, 102830.
11. Ho, A., Zhao, H., Fellowes, J. W., Martina, F., Davis, A. E., & Prangnell, P. B. (2019). On the origin of microstructural banding in Ti-6Al4V

wire-arc based high deposition rate additive manufacturing. *Acta Materialia*, *166*, 306-323.

12. A. Rouwane, “Strain localization in Ti and Ti-alloys using three-dimensional topographic imaging”, In Proceedings of the 15th World Conference on Titanium.
13. N. Maury, “Advances in the development of direct energy deposition for the manufacturing of aerostructures”, In Proceedings of the 15th World Conference on Titanium.
14. Liu, J. H., Vanderesse, N., Stinville, J. C., Pollock, T. M., Bocher, P., & Texier, D. (2019). In-plane and out-of-plane deformation at the sub-grain scale in polycrystalline materials assessed by confocal microscopy. *Acta Materialia*, *169*, 260-274.